Journal of the Nigerian Association of Mathematical Physics
***Volume* 19 (November, 2011), pp 499 – 512**

Verification of Positional Accuracy of ZVS3003 Geodetic Control Using CSSPS – PPP Model

R. Ehigiator – Irughe[1] and M. O. Ehigiator[2]

**[1]Department of Engineering Geodesy and Geomatics,
Siberian State Academy of Geodesy,
Novosibirsk, Russia.
[2]Department of Physics, Faculty of Basic Science,
Benson- Idahosa University, Benin City,
Nigeria.**

Abstract

The International GPS Service (IGS) has provided GPS orbit products to the scientific community with increased precision and timeliness. Many users interested in geodetic positioning have adopted the IGS precise orbits to achieve centimeter level accuracy and ensure long-term reference frame stability. Positioning with GPS can be performed by either of two ways: point positioning or differential (relative) positioning. GPS point positioning employs one GPS receiver, while differential positioning employs two (or more) GPS receivers simultaneously tracking the same satellites. Surveying works with GPS have conventionally been carried out in the differential positioning mode. This is mainly due to the higher positioning accuracy obtained with the differential positioning mode compared to that of the GPS point positioning. A major disadvantage of GPS differential positioning, however, is its dependency on the measurements or corrections from a reference receiver; i.e. two or more GPS receivers are required to be available. New developments in GPS positioning show that a user with a single GPS receiver can obtain positioning accuracy comparable to that of differential positioning (i.e., centimeter to decimeter accuracy). This work details a post-processing approach that uses un-differenced dual-frequency pseudorange and carrier phase observations along with IGS precise orbit products, for stand-alone precise geodetic point positioning (static or kinematic) with centimeter precision. This is possible if one takes advantage of the satellite clock estimates available with the satellite coordinates in the IGS precise orbit products and models systematic effects that cause centimeter variations in the satellite to user range. This paper will describe the approach, summarize the adjustment procedure and specify the earth and space based models that must be implemented to achieve centimeter level positioning in static mode. Results obtained using existing control as case studies are also presented.

1.0 Introduction

Canadian Spatial Reference System Precise Point Positioning (CSRS-PPP) uses the so-called point positioning approach (user doesn't need to be near an Active control points (ACP), IGS or continuous reference station (CORS). Unlike differential GPS methods, PPP does not require data from any other GPS receivers. Instead PPP uses precise apriori values of the GPS orbits and of their clocks. These values are obtained from the International GPS Service (IGS) and are usually available, in batches of 24 hours, 17 hours after the end of the GPS day. The precise orbits and clocks remove a large part of the GPS errors. In addition, PPP processing must also properly account for several other effects on the position of the GPS receiver.

Normally for dual frequency code and phase static data, PPP should provide cm level (1 or 2 in horizontal; 4 to 5 in vertical, anywhere in the world) accuracy after the phase ambiguities have been resolved which can require 30 to 90 minutes of data. Before the ambiguities can be resolved, the accuracy of the positions will be dependent only on the code observations.

Recently, precise point positioning (PPP) algorithms using un-differenced carrier phase observations have been added to software suites such as GIPSY and the traditional double-differencing BERNESE software. Users now have the option of processing data from a single station to obtain positions with centimeter precision within the reference frame provided by the IGS orbit products. Natural Resources Canada precise point positioning (NRCan PPP) software also evolved from its original

Corresponding authors: E-mail: raphehigiator@yahoo.com, geosystems_2004@yahoo.com , Tel. +2348055672620

version to provide increasing precision. Point positioning eliminates the need to acquire simultaneous tracking data from a reference (base) station or a network of stations. It has given rise to centralized geodetic positioning services that require from the user the simple submission of a request and valid GPS observation file.

The approach presented here is an implementation of precise point positioning that was effectively submitted data via internet to CSPR – PPP center for six (6) observations on ZVS300 from 2006 to 2011 using Trimble GPS and Leica GPS. Results obtained are consistent but did not agree with the existing GPS values. ZVS3003 was established in 1996 in the Niger Delta area of Nigeria and most of the surveys in Niger Delta are based on ZVS3003. Since the establishment of this control in 1996, no further investigation has been conducted with a view of finding out the integrity of the master control.

2.0 Precise Point Positioning

It has been shown that code-based point positioning solution could be improved to match the Differential Global positioning systems (DGPS) solution through the use of ionosphere-free, undifferenced pseudorange with precise ephemeris and clock data. To achieve the highest possible point positioning accuracy, both carrier-phase and pseudorange measurements should be used. In addition, the remaining unmodelled errors, namely tropospheric delay, satellite altitude error, and site displacement effect, must be dealt with. This approach is commonly known as the Precise Point Positioning, or PPP [1].

The ionospheric-free combinations of dual-frequency GPS pseudorange (P) and carrier-phase observations (Φ) are related to user position, clock, troposphere and ambiguity parameters according to the following simplified observation equations [1]:

$$\ell_P = \rho + C(dt-dT) + T_r + \varepsilon_P \qquad (1)$$

$$\ell_\phi = \rho + C(dt-dT) + T_r + N\lambda + \varepsilon_\Phi$$

where:

ℓ_P is the ionosphere-free combination of L1 and L2 pseudoranges ($2.54P_1-1.54P_2$),
ℓ_ϕ is the ionosphere-free combination of L1 and L2 pseudoranges ($2.54\phi_1-1.54\ \phi_2$),
dt is the station clock offset from GPS time,
dT is the satellite clock offset from GPS time,
C is the vacuum speed of light,
T_r is the signal path delay due to the neutral-atmosphere (primarily the troposphere),
λ is the carrier, or carrier-combination, wavelength,
N is the ambiguity of the carrier-phase ionosphere-free combination,
ε_P, is the relevant measurement noise components
ε_Φ multipath error

Symbol ρ is the geometrical range computed as a function of satellite (Xs, Ys, Zs) and station (x, y, z) coordinates according to:

$$\rho = (\Delta X^2 + \Delta Y^2 + \Delta Z^2)^{1/2} \qquad (2)$$

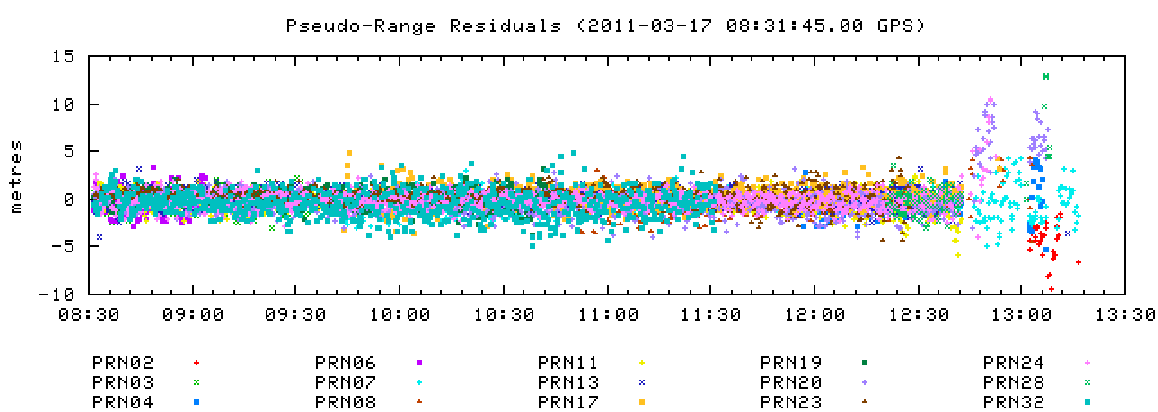

Figure 1 – Measured Pseudo – Range

Figure 1 is the Pseudo – Range result from the submitted GPS observation at ZVS3003. Cut off elevation in meter(m) was plotted against time of observation. Expressing the tropospheric path delay (T_r) as a function of the zenith p (zpd) and mapping function (*M*) and removing the known satellite clocks (*dT*) gives the following mathematical model in the simplest form [1]:

$$f_P = \rho + C\,dt + M\,zpd + \varepsilon_P - \square_P = 0 \qquad (3)$$
$$f_\Phi = \rho + C\,dt + M\,zpd + N\lambda + \varepsilon_\Phi - \square_\Phi = 0 \qquad (4)$$

3.0 Adjustment Model

Linearization of observation equations (3) and (4) around the a-priori parameters and observations (X^0,) becomes, in matrix form:

$$A\,\delta + W - V = 0, \qquad (5)$$

where *A* is the design matrix, δ is the vector of corrections to the unknown parameters *X*, $W = f(X^0, \ell)$ is the misclosure vector and *V* is the vector of residuals.

The partial derivatives of the observation equations with respect to *X*, consisting of four types of parameters:

station position (*x*,*y*,*z*), clock (*dt*), troposphere zenith path delay (*zpd*) and (non-integer) carrier-phase ambiguities (*N*), form the design matrix A[1]:

$$A = \begin{bmatrix} \frac{\partial f(X,\ell_p)}{\partial X_x} & \frac{\partial f(X,\ell_p)}{\partial X_y} & \frac{\partial f(X,\ell_p)}{\partial X_z} & \frac{\partial f(X,\ell_p)}{\partial X_{dt}} & \frac{\partial f(X,\ell_p)}{\partial X_{zpd}} & \frac{\partial f(X,\ell_p)}{\partial X_{N_{(j=1,nsat)}}} \\ \frac{\partial f(X,\ell_\Phi)}{\partial X_x} & \frac{\partial f(X,\ell_\Phi)}{\partial X_y} & \frac{\partial f(X,\ell_\Phi)}{\partial X_z} & \frac{\partial f(X,\ell_\Phi)}{\partial X_{dt}} & \frac{\partial f(X,\ell_\Phi)}{\partial X_{zpd}} & \frac{\partial f(X,\ell_\Phi)}{\partial X_{N^j_{(j=1,nsat)}}} \end{bmatrix} \qquad (6)$$

where

$$\frac{\partial f}{\partial X_x} = \frac{x - X_s}{\rho}, \quad \frac{\partial f}{\partial X_y} = \frac{y - Y_s}{\rho}, \quad \frac{\partial f}{\partial X_z} = \frac{z - Z_s}{\rho}$$

$$\frac{\partial f}{\partial X_{dt}} = C, \quad \frac{\partial f}{\partial X_{zpd}} = M, \quad \frac{\partial f}{\partial X_{N_{(j-1,nsat)}}} = 0$$

$$X = \begin{bmatrix} x \\ y \\ z \\ dt \\ zdt \\ N_{(j=1,nsat)} \end{bmatrix}$$

The least squares solution with *a-priori* weighted constraints (p_x) to the parameters is given by:

$$\delta = -\left(P_{X0} + A^T P_\ell A\right)^{-} A^T P_\ell W \qquad (7)$$

$$\bar{X} = X^0 + \delta \qquad (8)$$

with covariance matrix

$$C_{\bar{X}} = P_{\bar{X}}^{-1} = \left(P_{X^0} + A^T P_\ell A\right)^{-1} \tag{9}$$

4.0 Adjustment Procedure

The adjustment procedure developed is effectively a sequential filter that adapts to varying user dynamics. The implementation considers the variations in the states of the parameters between observation epochs and uses appropriate stochastic processes to update their variances. The current model involves four types of parameters: station position (*x, y, z*), receiver clock (*dt*), troposphere zenith path delay (*zpd*) and carrier-phase ambiguities (*N*). The station position may be constant or change over time depending on the user dynamics. These dynamics could vary from tens of meters per second in the case of a land vehicle to a few kilometers per second for a low earth orbiter (LEO). The receiver clock will drift according to the quality of its oscillator, e.g. several centimeters/second in the case of an internal quartz clock with frequency stability of about 10^{-10}. Comparatively, the zenith path delay will vary in time by a relatively small amount, in the order of a few centimeters/hour. Finally, the non-integer carrier-phase ambiguities (*N*) will remain constant as long as the carrier phases are free of cycle-slips, a condition that requires close monitoring. (Note that for double differenced data, (*dt)* is practically eliminated and the carrier-phase ambiguities *(N)* become integers).

Using subscript *i* to denote a specific time epoch, we see that without observations between epochs, initial parameter estimates at epoch *i* are equal to the ones obtained at epoch *i-1*[1]:

Hence,

$$X_i^0 = \bar{X}_{i-1} \tag{10}$$

To propagate the covariance information from epoch *i-1* to *i*, during an interval Δt, it has to be updated to include process noise represented by the covariance matrix $C\varepsilon_{\Delta t}$

Thus,

$$P_{X_i^0} = \left[C_{\bar{X}\,i-1} + C\varepsilon_{\Delta t}\right]^{-1} \tag{11}$$

where

$$C\varepsilon_{\Delta t} = \begin{bmatrix} C\varepsilon(x)_{\Delta t} & 0 & 0 & 0 & 0 & 0 \\ 0 & C\varepsilon(y)_{\Delta t} & 0 & 0 & 0 & 0 \\ 0 & 0 & C\varepsilon(z)_{\Delta t} & 0 & 0 & 0 \\ 0 & 0 & 0 & C\varepsilon(dt)_{\Delta t} & 0 & 0 \\ 0 & 0 & 0 & 0 & C\varepsilon(zpd)_{\Delta t} & 0 \\ 0 & 0 & 0 & 0 & 0 & C\varepsilon(N^j_{(j=1,nsat)\,\Delta t} \end{bmatrix}$$

4.1 Precise Point Positioning Correction Models

Developers of GPS software are generally well aware of corrections they must apply to pseudorange or carrier-phase observations to eliminate effects such as special and general relativity, Signal delay, satellite clock offsets, atmospheric delays, etc. All these effects are quite large, exceeding several meters, and must be considered even for pseudorange positioning at the meter precision level. When attempting to combine satellite positions and clocks precise to a few centimeters with ionospheric-free carrier phase observations (with millimeter resolution), it is important to account for some effects that may not have been considered in pseudorange or precise differential phase processing modes [8].

Other additional correction terms that are significant for carrier phase point positioning are under *Satellite Altitude Effects*, *Site Displacements Effects* and *Compatibility Considerations*. A number of the corrections listed above require the Moon or the Sun positions which can be obtained from readily available planetary ephemerides files, or more conveniently from simple formulas [8].

4.2 Kinematic Positioning Algorithm

The steps followed by the relative kinematic positioning algorithm developed by NAVSYS are illustrated in Figure 1. Kinematic positioning and alignment relies on the relationship of the carrier phase observations to the range observations described by the following equation [2].

$$
\begin{aligned}
PR_1 &= R + bu_1 + bsv_{PR\,1} + T + I_1 + {}_{nPR\,1} \\
PR_2 &= R + bu_2 + bsv_{PR\,2} + T + I_1 \frac{\lambda_2^2}{\lambda_1^2} + {}_{nPR\,2} \\
-CPH_1 &= R + bu_{CPH\,1} + bsv_{CPH\,1} + T - I_1 + {}_{nCPH\,1} - N_1\lambda_1 \\
-CPH_2 &= R + bu_{CPH\,2} + bsv_{CPH\,2} + T - I_1 \frac{\lambda_2^2}{\lambda_1^2} + {}_{nCPH\,2} - N_2\lambda_2
\end{aligned}
\tag{12}
$$

Where

PR = pseudo-range on L1 or L2 frequencies (meters), CPH = carrier phase on L1 or L2 frequencies, (meters), RT = true range (meters), bu = range equivalent receiver clock offset (meters), bsv = range equivalent satellite clock offset (meters)

T = tropospheric delay (meters), I = ionospheric delay (meters), n = measurement noise (meters), N = CPH integer (cycles), λ = carrier wavelength (meters)

The ionospheric delay is different on the L1 and L2 observations as it is inversely proportional to the frequency squared and so can be removed from the PR by differencing. The DGPS corrections will remove any errors in the navigation solution caused by satellite position and clock offsets. The accuracy of the PR derived DGPS corrected position solution is a function of the pseudo-range noise, which includes receiver noise and multipath errors. The GPS/inertial navigation solution will filter the short-term noise effects, but it cannot correct for correlated noise errors from multipath.

The major problem with static GPS is the time required for an appreciable change in the satellite/receiver geometry so that the initial integer ambiguities can be resolved. However, if the integer ambiguities could be resolved (and constrained in a least squares solution) prior to the survey, then a single epoch of data would be sufficient to obtain relative positioning to sub-centimeter accuracy. This concept is the basis of kinematic surveying. It can be seen from this that, if the integer ambiguities are resolved initially and quickly, it will be necessary to keep lock on these satellites while moving the antenna [1].

4.3 Resolving the integer ambiguities

The process of resolving the integer ambiguities is called 'initialization' and may be done by setting-up both receivers at each end of a baseline whose coordinates are accurately known. In subsequent data processing, the coordinates are held fixed and the integers determined using only a single epoch of data. These values are now held fixed throughout the duration of the survey and coordinates estimated every epoch, provided there are no cycle slips. The initial baseline may comprise points of known coordinates fixed from previous surveys, by static GPS just prior to the survey, or by transformation of points in a local coordinate system to WGS 84 [3].

The ambiguity should be constant as long as the receiver is locked to the signal. Theambiguity number changes when the receiver loses lock. Unlike the double differenced carrier phase, the undifferenced PPP analysis estimates only real numbers of ambiguities, or floated solutions. In fact, PPP ambiguities are reparameterized ambiguities which are collections of ambiguities of L1 and L2, with carrier phase ionosphere-free scaling factors. Figure 2 is the Ambiguities resolution from the submitted GPS observation at station ZVS3003. Table 2 shows cut off elevation with time.

The reparameterized ambiguities $(\bar{N})$ are being estimated every epoch, as a pure random walk process. The dynamic model is in the form:

$$
\bar{N}^{P}_{i+1} = N_i^P + w \tag{13}
$$

where *w* is Gaussian noise.

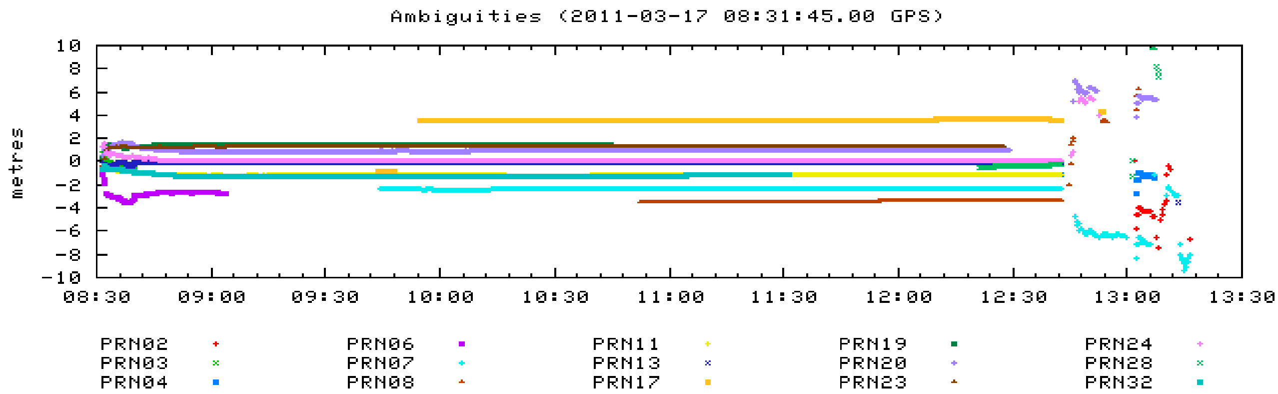

Figure 2 – Ambiguities Resolution at ZVS3003

5.0 Code Measurement

The GPS code measurement ρ is a linear measurement known as pseudo range in meters. Pseudo Range is a measure of the distance between the satellite and receiver at the time epoch of transmission and reception of the signals.

The transmit time of the signals is measured by comparing (correlating) identical Pseudo Random Noise (PRN) codes generated by the satellite and the receiver [6].

$$\rho = R + C\,(dt - dT) + d_{ion} + d\,t_{rop} + d_{mpath.} \qquad (14)$$

where

R = True range between the SV (at transmit time) and receiver (at r receiver time)

d_{ion}= Ionospheric delay parameter

dt_{rop}= Measurement delay due to troposphere (m)

d_{mpath} = Measurement delay due to multipath

Most DGPS Processing involves generating a nominal “computed” range between the receiver and the satellite which is calculated from the known coordinate of the receiver locations and the satellite [4].

The true range vector **R** is

$$\mathbf{R} = P_{sv} - P_{rec} \qquad (15)$$

Where; P_{sv} – is the computed position of the satellite at transmit time (From ephemeris)

P_{rec} is the nominal position of the receiver at receiver time.

5.1 Carrier Measurement

The constant motion of the GPS satellite constellation in orbit demands that the receiver be capable of taking care of the changing Doppler frequency shift on L_1.

In the case of Dual frequency receivers both L_1 and L_2 are tracked. L_1 wavelength is 19cm and L_2 wavelength is 24cm. The shift in frequency arises due to the relative motion between the satellite and the receivers. Integration of the Doppler frequency offset results in an extremely accurate measurement of the advance in signal carrier phase between time epochs [4].

Using Double Differencing Processing DD techniques on C/A or P(Y) – code carrier phase observables removes most of the error sources.

To achieve centimeter level accuracy, it is still necessary to carry out further refinement of the propagation path length measurement using carrier – cycle integer ambiguity resolution.

Once the receiver locks on to a particular satellite, it not only make C/A and or p(Y) code pseudo range measurements on L_1 and L_2 (if L_2 is present) but it also keeps a running count based upon the Doppler frequency shift present on L_1 and L_2 carrier frequencies.

Each epoch for running this cycle count is available for the receiver. It should be noted that the advance in carrier phase during an epoch is determined by integrating the carrier Doppler Frequency offset (fo) over the interval of the epoch. Frequency fo is the time rate of change of the carrier phase, hence integration over an epoch yields, the carrier phase advance during an epoch. At the conclusion of each epoch, a fractional phase measurement is made by the receiver. This measurement is derived from the carrier phase tracking loop of the receiver. Mathematically the relationship is as follows [4]:

$$\phi_{1.1n} = \phi_{1.1n-1} = \int_{I_{n-1}}^{In} f_{0_{1.1}}(r)dr + \phi_{1.10}$$

$$Where \quad \phi_{1.10} = 0$$

$$\phi_{1.2n} = \phi_{1.2n-1} = \int_{I_{n-1}}^{In} f_{o_{1.2}}(r)dr + \phi_{1.20}$$

$$Where \quad \phi_{1.20} = 0 \qquad (16)$$

Where

ϕ is the accumulated phase at the epoch shown
n and n-1 are the current and immediate past epochs
f_D - is the Doppler frequency as a function of time
ϕ_1 is the fractional phase measured at the epoch shown

Figure 3 is the Carrier - Phase result from the submitted GPS observation at ZVS3003. The observation residuals and phase ambiguities graphical output consists in a series of plots of observations (pseudoranges and/or carrier phase) and carrierphase ambiguities versus time. Similarly to the estimated parameters plots, the
resolution may only allow for averaged values to be plotted
.

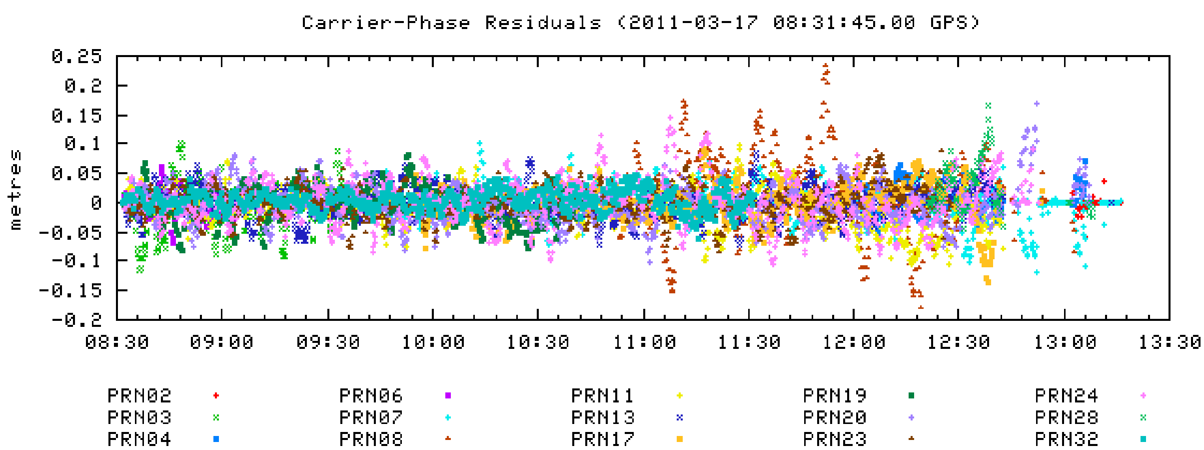

Figure 3 – Carrier - Phase Measurement

5.2 Ionospheric Delay

The ionosphere is the part of the upper atmosphere where free electrons occur in sufficient density to have an appreciable influence on the propagation of radio frequency electromagnetic waves. It is a weak ionized plasma extending from approximately 50Km to 1000Km above the surface of the earth and can affect radio wave propagation in various ways [3].
Ionosphere is a dispersive medium. The refractive index is a function of the operating frequency. The refractive index n of the ionosphere can be expressed as [4].

$$n^2 = 1 - \frac{X}{1 - iZ - \frac{Y_\tau^2}{2(1 - X - iZ)} \pm \left[\frac{Y_\tau^4}{4(1 - X - iZ)^2} + Y_L^2\right]^{1/2}}$$

Where (17)

$$X = \frac{N_e e^2}{\varepsilon_n m \omega^2} \qquad ; Y_L = f_H \frac{Cos\ \theta}{f} \qquad ; Y_\tau = f_H \frac{\sin\ \theta}{f}$$

$$Z = \frac{v}{w} \qquad ; w = 2\Pi f$$

and

f	-	is frequency of incoming signal in Hz
N_e	-	is the electron density in electron / m^3
e	-	is the electron charge = -1.602 X 10^{-19} Coulomb
ε_n	-	is the permittivity of free space = -8.854 X 10^{-12} Farad / m
m	-	is the rest mass of electron = 9.107 X 10^{-31} Kg
Θ	-	is the angle of the ray with respect to the earth's magnetic field.
V	-	is the electron – neutron collision frequency and
f_H	-	is the electron gyro frequency typically 1.5MHz

5.3 TROPOSPHERIC DELAY

Tropospheric delay occurs as a result of the GPS signals passage through the Earth's lower atmosphere. This region extends to an altitude approximately 10km above the earth's surface. The stratosphere is also considered part of the lower atmosphere. It extends upward from the tropopause to an altitude of approximately 50 kilometers in these two sections of the atmosphere, electromagnetic refraction slows the GPS radio signals causing a delay in its arrival at the receiver [4]. Figure 4 shows five hours' time series obtained from PPP for station ZVS3003 during GPS observation using precise orbit products.

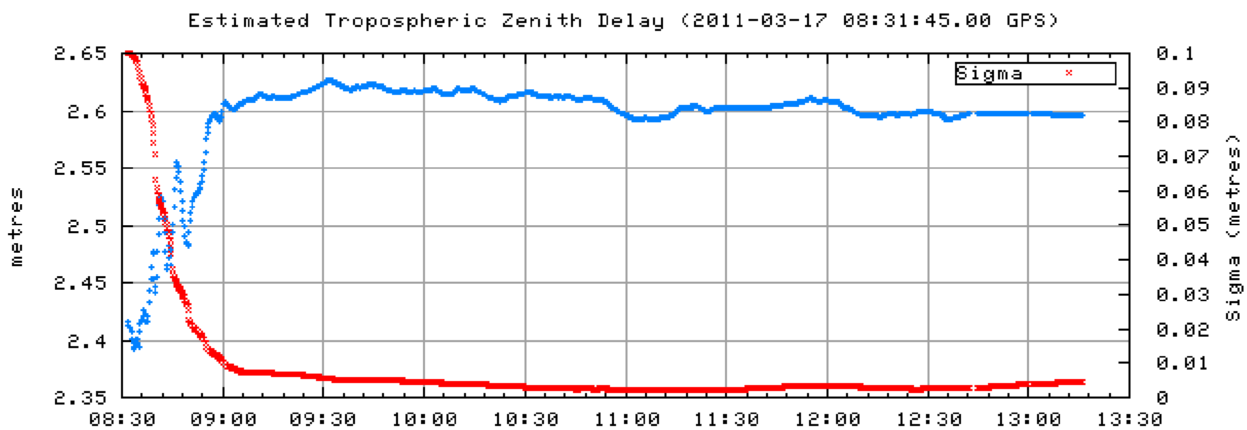

Figure 4 – Estimated Troposphere measurement

5.4 Receiver Noise

Receiver noise can be considered as white noise as it is uncorrelated over time. In the case of GPS, it is the error in phase and code measurement due to imperfect tracking of the GPS signals by the phase and delay lock loops. The tracking error is random and is assumed to have a Gaussian distribution. The magnitude of the noise is a function of the measurement type and the signal strength [4].

The C/A – code measurement can be tracked with a typical accuracy of 1.5 meters but it may vary between 0.2 and 3 meter depending upon the strength of the receiver signal. Typical receiver noise for P(Y) code measurement is 10 – 30cm. Code and carrier phase measurement noise can be smoothed by an estimate of a "zero baseline" test [6].

The GPS signal is split into two and fed to two separate but same types of receivers. In static application, the predominant error component in carrier phase noise is jitter of the phase lock loop caused by thermal noise. This can be expressed according to; [4]

$$\sigma_n = \sigma_{PLL} = \frac{\lambda}{2\pi}\sqrt{\frac{B_n}{C/\ n_o}\left(1+\frac{1}{\frac{2TC}{n_o}}\right)} \quad meters \qquad (18)$$

where

B_n	-	carrier loop noise band width in Hz
$\frac{C}{n_{io}}$	-	is the carrier to noise power expressed as $10^{C/No/10}$ with C/No in dB - Hz
T	-	is the predetections integration time in seconds
λ	-	is carrier wavelength

5.5 Receiver Clock Estimation

Receiver clock can be estimated using a Gauss-Markov process. Suggested that the receiver clock can be modeled as white noise. However, it is better to model it as random walk. Since we have pseudorange observations which include the clock term, an approximate ratio of the change in the clock from the current epoch. The dynamic model can be directly expressed as;

$$R_i = P_i^p - (\rho_i^p - cdt_i^p)$$

$$R_{i+1} = P_{i+1}^p - (\rho_{i+1}^p - cdt_{i+1}^p) \tag{19}$$

$$\Phi_{clk} = \frac{R_{i+1}}{R_i} \tag{20}$$

Because many satellites are observed at the same time, it is additionally better to average out the random error by averaging the ratio of all available satellites. The PPP solution obtained from the random walk process with a priori information of the ratio of receiver clock shows a slight solution improvement than that using the white noise process.

Satellite orbit errors result from the uncertainty in orbital information. To compute the satellite position, we either use broadcast ephemeris or precise ephemeris. Although precise ephemeris information is much more accurate than those of broadcast information. The satellite positions are computed from a set of Keplerian orbit and perturbation parameters with clock parameters which are predicted states for the satellite orbit and are updated every two hours [1]. Figure 5 is the linear residual of Station Clock result from the submitted GPS observation to CSSPS – PPP for station ZVS3003.

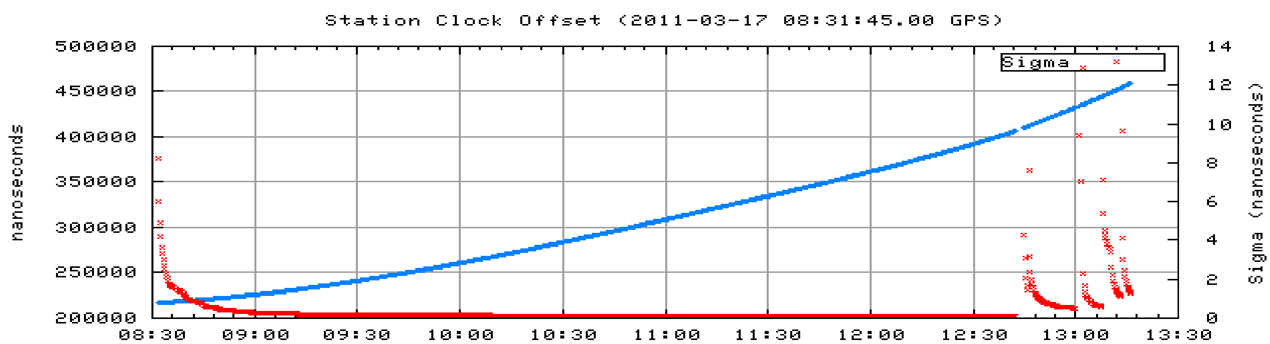

Figure 5 – Station Clock offset

5.6 Multi Path

Multi path refers to the existence of signals reflected from objects in the vicinity of a receiver's antenna that corrupt the direct line-of-sight signals from the GPS satellites, thus degrading the accuracy of both code-based and carrier phase-based measurements. The object may be tall buildings, television and Telephone masks, etc

6.0 PPP Solution Convergence

PPP convergence as a function of time depends on initial parameter variances and the synergy of GPS pseudorange and carrier phase observations. At the initial epoch, because of unknown carrier-phase ambiguities, the solution relies entirely on the pseudorange observations and the quality of the position reflects GPS receiver code resolution and the multipath environment at the tracking station. As time passes and phase observations are added to the solution, the ionospheric free ambiguities and station position components (in static mode) converge to constant values while the troposheric zpd and receiver clock parameters vary as a function of their assigned process noise. Figure 6 shows the linear residual of Latitude difference, Longitude difference, and Ellipsoidal difference for station ZVS3003.

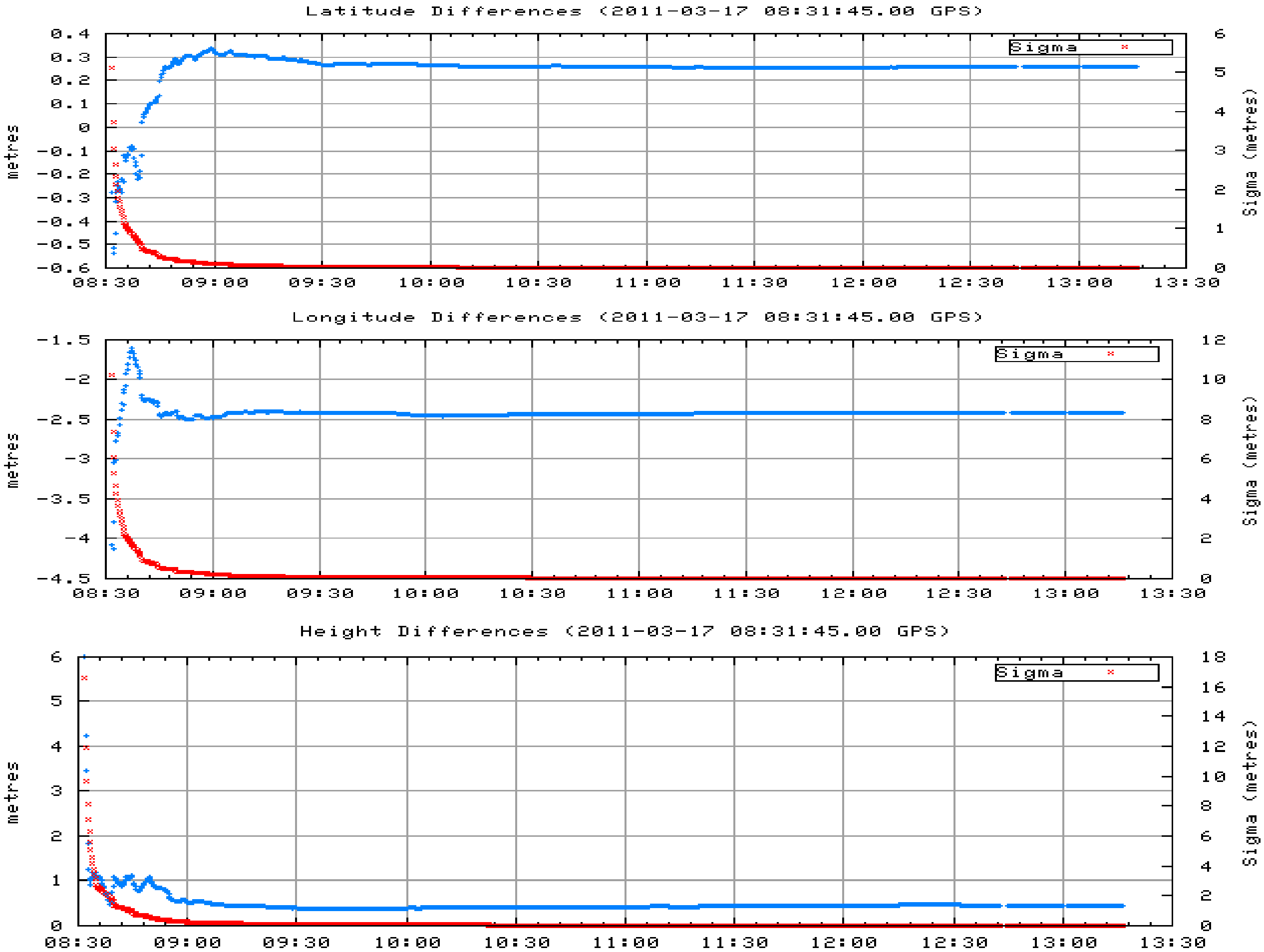

Figure 6 - Solution convergence

Figure 6 shows the latitude; Longitude and Ellipsoidal Height for 2011 using Trimble 5800 receiver on ZVS300. Figure 7 is the Pseudo – Range sky distribution of satellite, while figure 8 is the Ellipsoidal profile of station ZVS3003

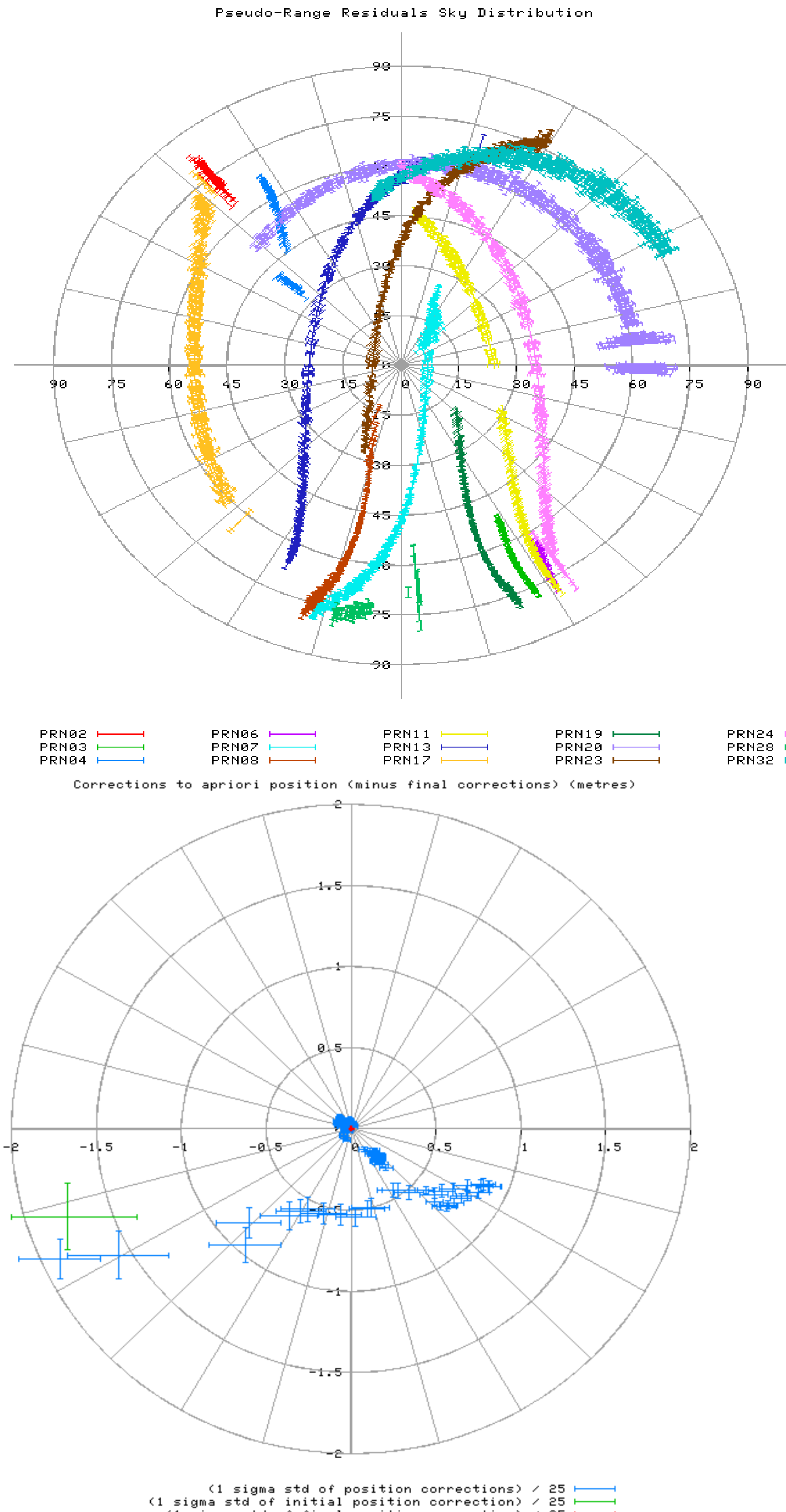

Figure 7- Pseudo – Range and Apriori correction

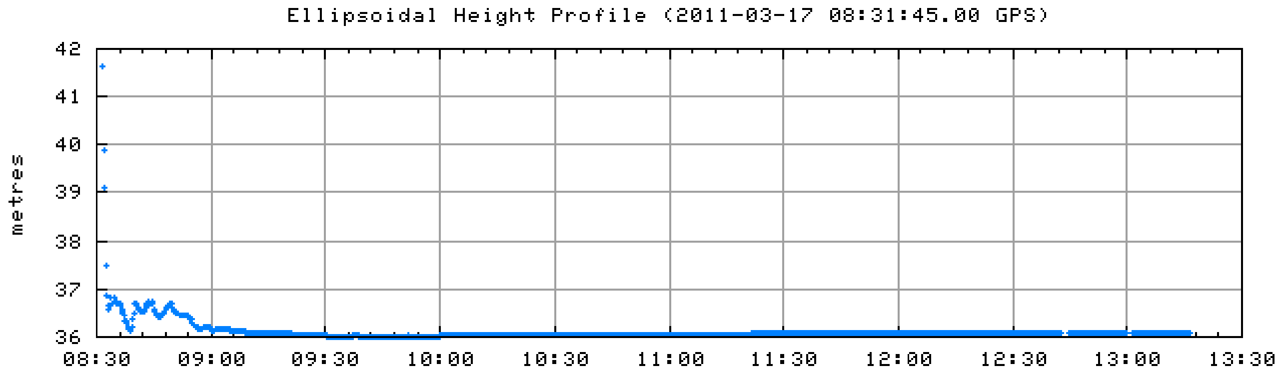

Figure 8 – Ellipsoidal Height Profile

6.1 Results Of Adjustments Of Observations

The qualities to be obtained after field measurements and adjustment in a GPS network include baseline vector components and their covariance. We present in Table 1 summary of the coordinates obtained using CSRS- PPP online processing results.

Six (6) GPS observation were carried out between 2006 and 2011 using two different GPS Receivers at station ZVS3003 located in Port Harcourt Nigeria. Leica SR399 Internal L1/L2 Receiver was used in 2006 and 2011 respectively, while Trimble 4000SSI L1/L2 was used in 2008 and Trimble 5800 L1/L2 receiver in 2011. The results obtained using CSRS – PPP was compared with the existing GPS value and are presented in Table 1 below. For 2006 result, ΔN was found to be 0.885m, while ΔE was found to 2.775m. 2D and 3D displacements were found to be 2.913m and 3.305m. 2008 result reveal ΔN to be 0.916m and ΔE is 2.77m. 2D and 3D values were found to be 2.922m and 3.268m. For 2011, ΔN is 0.947m, ΔE is 2.65m while 2D and 3D values were found to 2.819m and 4.145m respectively. The respective accuracy standard (standard Deviation) for the observation was also presented and they appear consistent within few centimeters. Leica GPS data for 2011 was rejected due to decrease in accuracy standard. The accuracy standard was found to be 0.224m in Latitude, 0.438m Longitude and 0.877m in the Ellipsoid. This resulted to a higher 2D and 3D displacement.

The results show consistent shift in the south – East and North – West in all the observations. We cannot conclude yet if the station has positional error till more observations is carried out using CORS in Nigeria as reference point.

Table 1 – GPS Coordinate Values Comparison for ZVS3003

INSRT.	CSPS - PPP WGS84 VALUE						EXISTING WGS84 VALUE			CSRS - PPP MINNA VALUE		EXISTING MINNA VALUE		DISPLACEMENT	
	LAT	LONG	ELLIP(m)	STANDARD DEVIATION(m)			LAT	LONG	ELLIP(m)	NORTHING	EASTING	NORTHING	EASTING	?N	?E
LEICA GPS: Year 2006	4 50 52.6738	7 02 52.0681	36.222	0.012	0.039	0.063	4 50 52.70302	7 02 52.15767	37.783	93842.484	509561.66	93843.369	509564.435	-0.885	-2.775
										$\left(\sqrt{(\Delta N^2)+(\Delta E^2)}\right)$		$\left(\sqrt{(\Delta N^2)+(\Delta E^2)+\Delta H^2}\right)$			
										2.913			3.305		
TRIMBLE GPS: Year 2008	4 50 52.6733	7 02 52.0685	36.32	0.07	0.019	0.061	4 50 52.70302	7 02 52.15767	37.783	93842.453	509561.66	93843.369	509564.435	-0.916	-2.775
										$\left(\sqrt{(\Delta N^2)+(\Delta E^2)}\right)$		$\left(\sqrt{(\Delta N^2)+(\Delta E^2)+\Delta H^2}\right)$			
										2.922			3.268		
TRIMBLE GPS: Year 20111	4 50 52.6735	7 02 52.0628	36.08	0.005	0.014	0.026	4 50 52.70302	7 02 52.15767	37.783	93842.484	509561.814	93843.369	509564.435	-0.885	-2.621
										$\left(\sqrt{(\Delta N^2)+(\Delta E^2)}\right)$		$\left(\sqrt{(\Delta N^2)+(\Delta E^2)+\Delta H^2}\right)$			
										2.766			3.249		
TRIMBLE GPS: Year 20111	4 50 52.6720	7 02 52.0722	34.741	0.022	0.063	0.089	4 50 52.70302	7 02 52.15767	37.783	93842.422	509561.783	93843.369	509564.435	-0.947	-2.652
										$\left(\sqrt{(\Delta N^2)+(\Delta E^2)}\right)$		$\left(\sqrt{(\Delta N^2)+(\Delta E^2)+\Delta H^2}\right)$			
										2.816			4.145		
LEICA GPS: Year 2011	4 50 52.6732	7 02 52.0681	36.15	0.013	0.04	0.058	4 50 52.70302	7 02 52.15767	37.783	93842.453	509561.66	93843.369	509564.435	-0.916	-2.775
										$\left(\sqrt{(\Delta N^2)+(\Delta E^2)}\right)$		$\left(\sqrt{(\Delta N^2)+(\Delta E^2)+\Delta H^2}\right)$			
										2.922			3.348		
LEICA GPS: Year 2011	4 50 52.6269	7 02 52.0873	26.957	0.224	0.438	0.877	4 50 52.70302	7 02 52.15767	37.783	93841.039	509562.242	93843.369	509564.435	-2.33	-2.193
										$\left(\sqrt{(\Delta N^2)+(\Delta E^2)}\right)$		$\left(\sqrt{(\Delta N^2)+(\Delta E^2)+\Delta H^2}\right)$			
					REJECTED OBSERVATION					3.200			11.289		

Table 2.Processing Summary of one of the observation at ZVS3003

CSRS-PPP

(Processing Software Version: 1.04 1087)

Processing Summary for 05880760.11o

Data Start		Data End
2011-03-17 08:31:45.00		2011-03-17 13:16:15.00
Apri / Aposteriori Phase Std		**Apri / Aposteriori Code Std**
0.015m / 0.013m		2.0m / 1.132m
Observations	**Frequency**	**Mode**
Phase and Code	L1 and L2	Static
Elevation Cut-Off	**Rejected Epochs**	**Estimation Step**
10.000 degrees	1.32 %	Same as Input RINEX File
Antenna Model	**APC to ARP**	**ARP to Marker**
TRM41249.00	L1= 0.055 m L2= 0.057 m	-0.000 m

(APC = antenna phase center; ARP = antenna reference point)

Estimated Position for 05880760.11o

	Latitude (+n) (dms)	Longitude (+e) (dms)	Ell. Height (m)
NAD83(CSRS) (2011)	4 50 52.6735	7 02 52.0728	36.080
Sigmas	0.005 m	0.014 m	0.026 m
Apriori	4 50 52.665	7 02 52.151	35.635
Estimated - Apriori	0.261 m	-2.411 m	0.446 m
Orthometric Height CGVD28 (HTv2.0)	_NOT_DEFINED_	(click here for model and accuracy)	

(Coordinates from RINEX file used as apriori position)

7.0 Discussion and Conclusion

The observation equations, estimation technique and station/satellite models used for the implementation of GPS precise point positioning using IGS orbit/clock products were described. A post-processing approach that uses dual-frequency pseudorange and carrier-phase observations from a single GPS receiver and estimates station coordinates, tropospheric zenith path delays and clock parameters was developed. Results show that global centimeter positioning precision can be realized, directly in ITRF, when using precise orbits/clock products from different IGS Analysis Centres (ACs) and the IGS combinations.

The single point positioning mode presented here forms an ideal interface to the IGS orbit/clock products and ITRF. The approach is equally applicable to global kinematic positioning/navigation at the cm-dm precision level.

REFERENCES

[1] Jan Kouba and Pierre Héroux (2010), GPS Precise Point Positioning Using IGS Orbit Products, Paper presented at Geomatics'2010, Ottawa, Ontario, Canada,June 13-15.

[2] Andrew W. Sutter, Alan G. Evans (2004). Evaluation of Precise, Kinematic GPS Point Positioning. Proceedings of the Institute Of Navigation (ION) GNSS-2004 Meeting, Long Beach, California, USA.

[3] Schoffield, W. (1993) “Engineering Surveying”. Butterworth –Heinemann Ltd, Oxford, London.

[4] W. Schofield. Engineering Surveying; Theory and Examination Problems for Students, Fifth Edition Kingston University, London.

[5] CSRS-PPP (NRCANGSD)**-** Service Provided by Natural Resource, Canada. http://www.geod.nrcan.gc.ca/products-produits/ppp_e.php.

[6] Ehiorobo O.J (2008) “ Robustness analysis of a DGPS network for Earth Dam Deformation Monitoring”. PhD thesis, department of Civil Engineering, University of Benin, Benin City Nigeria.

[7] Gao, Y and Chen, K. (2001) “ Improving Ambuiguity Convergence in Carrier Phase Based Precise Point Positioning'', Proceedings 10N, GPS 2001, Salt Lake City, Utah.

[8] Gao, Y and Chen,K (2002) “ A New Method for Carrier Phase Based Precise Point Positioning'' Navigation, Journal of the Institute of Navigation Vol 49, No. 2.

[9] Gao Y and Chen K (2005) “ Performance analysis of precise point positioning using real time orbit and clock products” Journal of Global positioning system Vol 3 No 1-2 pp95-100.

[10] Raquet, F. J. (1998) “ Development of a method of kinematics GPS carrier phase ambiguity resolution using multiple reference receivers” Ph.D Dissertation, Department of Geomatics Engineering, Schulich School of Engineering, University of Calgary, Alberta, Canada.

[11] Abdel-Salam, M. (2005) “Precise point positing using un-differenced code and carrier phase observation”. Ph.D dissertation, Department of Geomatics Engineering, Schulich School of Engineering, University of Calgary, Alberta, Canada.

[12] Ahmed El-Rabbany,(2002), Precise GPS Point Positioning: the Future Alternative to Differential GPS. Surveying Proceedings of the ION GPS-2002, Oregon Convention Centre, Portland, Oregon, USA, September 24-27

[13] On-line Precise Point Positioning (2004). How To Use Document, Natural Resources Canada**.** Canada Centre for Remote Sensing Geodetic Survey Division. www.geod.nrcan.gc.ca